2025 SCEC Final Report, Project #25290

Incorporating Abundant Earthquake Data from Densified Permanent Seismic Networks and Temporary Nodal Array into Local Earthquake Tomography to Improve 3-D Seismic Velocity Structure in the Mendocino Triple Junction Region

PI: Hao Guo
University of Wisconsin-Madison

1. Objectives

The Mendocino Triple Junction (MTJ) region in northern California is one of the most seismically active regions in the U.S. A high-resolution 3-D seismic velocity model is essential for assessing seismic hazard in the MTJ region. The main goals of this project include: (1) improve an existing 3D velocity model of Guo et al. (2021) by incorporating more local earthquake data to take advantage of the permanent seismic networks densified in recent years and a dense nodal array deployed in 2020, aiming to better characterize downdip variations in material properties from the locked zone to the transition zone; and (2) use the improved model to relocate two recent magnitude 6 earthquake sequences (2021/12/20 M6 Petrolia and 2022/12/20 Mw 6.4 Ferndale sequences) to study the seismogenesis and fault structures of these two moderate earthquakes.

We have determined new velocity models using the triple-difference seismic tomography method by incorporating abundant local earthquake data since 2016 into the tomographic inversion of Guo et al. (2021). The new model shows decrease in Vp/Vs from the locked zone to the transition zone, suggesting significant decrease in porosity and fluid content that may be correlated with the brittle-to-ductile transition. The new model shows very high Vp/Vs in the accretionary wedge, indicating it is a fluid-rich, sedimentary region. Using the new velocity model, we relocated two template matching catalogs and one deep learning catalog of the 2021 and 2022 M6 sequences, which show spatial relationships between mainshock rupture, aftershock distribution, and Vp/Vs structures.

2. Data and Methodology

We combined the original data of Guo et al. (2021) and our newly collected data for seismic tomographic inversion. The original data of Guo et al. (2021) cover both the onshore and offshore regions. Their offshore data are from two dense ocean bottom seismometer (OBS) arrays deployed during 2012-2015 as a part of the Cascadia Initiative (Toomey et al., 2014) (Fig. 1). Their onshore data contain earthquakes data from 1984 to 2015 on permanent seismic networks, i.e., stations from Northern California Earthquake Data Center NCEDC (NCEDC, 2014), and a temporary network XQ deployed during 2007-2009 (Levander, 2007) (Fig. 1). Our newly collected data include 2559 local earthquakes since 2016 from the NCEDC catalog, recorded by permanent NCEDC stations and a temporary nodal array called the Southern Cascadia Earthquake and Tectonics Array (SCENTAR). SCENTAR was deployed in March-April 2020 by researchers at Purdue University and the University of Oregon (Delph et al., 2022). This array consists of 60 three-component nodal seismometers with an average station spacing of ~15 km, and stations recorded ~38 days of data (Fig. 1). Fig. 1 shows all the earthquakes and stations we used.

We used the triple-difference seismic tomography method (tomoTD), developed by Guo et al. (2021) based on the widely used double-difference tomography method (tomoDD, Zhang & Thurber, 2003), to jointly invert event locations and 3D velocity model. By using absolute arrival time data and the event-pair and station-pair differential time data, tomoTD can simultaneously determine high-precision absolute and relative event locations and high-resolution velocity structures in both earthquake source regions and the regions beneath seismic stations (Share et al., 2019; Guo et al., 2021).

Using our new 3D velocity model, we relocated three existing catalogs of the 2021 Petrolia and 2022 Ferndale M6 earthquake sequences with the triple-difference seismic location method of Guo & Zhang

(2017). These catalogs include the template matching catalog of the 2021 Petrolia M6 sequence developed by Yeck et al. (2023), the template matching catalog of the 2022 Ferndale M6 sequence developed by Shelly et al. (2024), and the deep learning catalog of earthquakes between 1 December 2021 and 1 June 2023, covering both of the 2021 and 2022 M6 sequences, developed by Yoon & Shelly (2024). These catalogs are much more complete compared to the NCEDC catalog. However, these catalogs were located using a 1-D velocity model, which could bias both absolute and relative locations, especially the former in the depth direction. We used the triple-difference seismic location method (hypoTD) of Guo & Zhang (2017), which can determine high-precision absolute and relative event locations by using station-pair and double-pair differential time data, especially when a 3-D velocity model is available to use. We obtained catalog phase arrival times and event-pair WCC differential arrival times of Yeck et al. (2023), Shelly et al. (2024), and Yoon & Shelly (2024) shared by Dr. David Shelly and Dr. Clara Yoon. These data were used to construct the station-pair and double-pair differential time data for the hypoTD location inversion.

In addition, we relocated 58 low-frequency earthquakes (LFEs) of Plourde et al. (2015) with our new velocity model using the triple-difference location method.

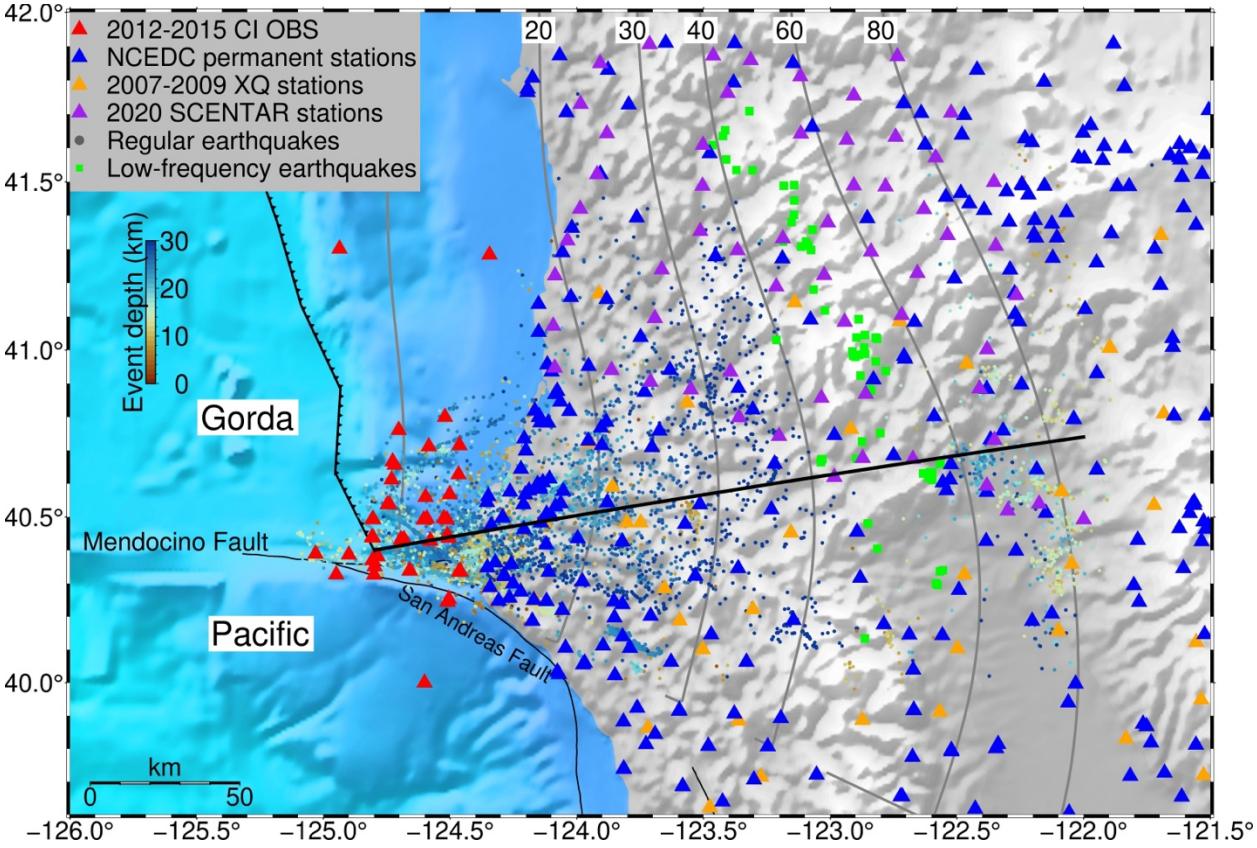

Figure 1. Earthquakes and stations in the MTJ region used for the seismic tomographic inversion in this project. Dots represent regular earthquakes, colored by focal depths. Triangles represent permanent and temporary seismic network stations, as labelled in the legend. Also shown are low-frequency earthquakes (green rectangles). The black sawtooth line represents the deformation front. Gray lines represent the depth contours of the Gorda slab interface from the Slab2 model (Hayes et al., 2018). The Mendocino Fault and San Andreas Fault are also shown as black lines. The black line trending NNE direction from the deformation front to the east of low-frequency earthquakes shows the profile of the cross-section shown in Fig. 2.

3. Results

3.1 New Velocity Model

Our tomographic inversion achieves significant reduction in data residual. The catalog data residual decreases from 0.252 s to 0.108 s and the WCC data residual decreases from 0.179 s to 0.028 s. Our new Vp, Vs, and Vp/Vs models are present in Fig. 2, which shows an along-dip cross-section. We conducted checkerboard test to assess model resolution and masked low-resolution regions in Fig. 2.

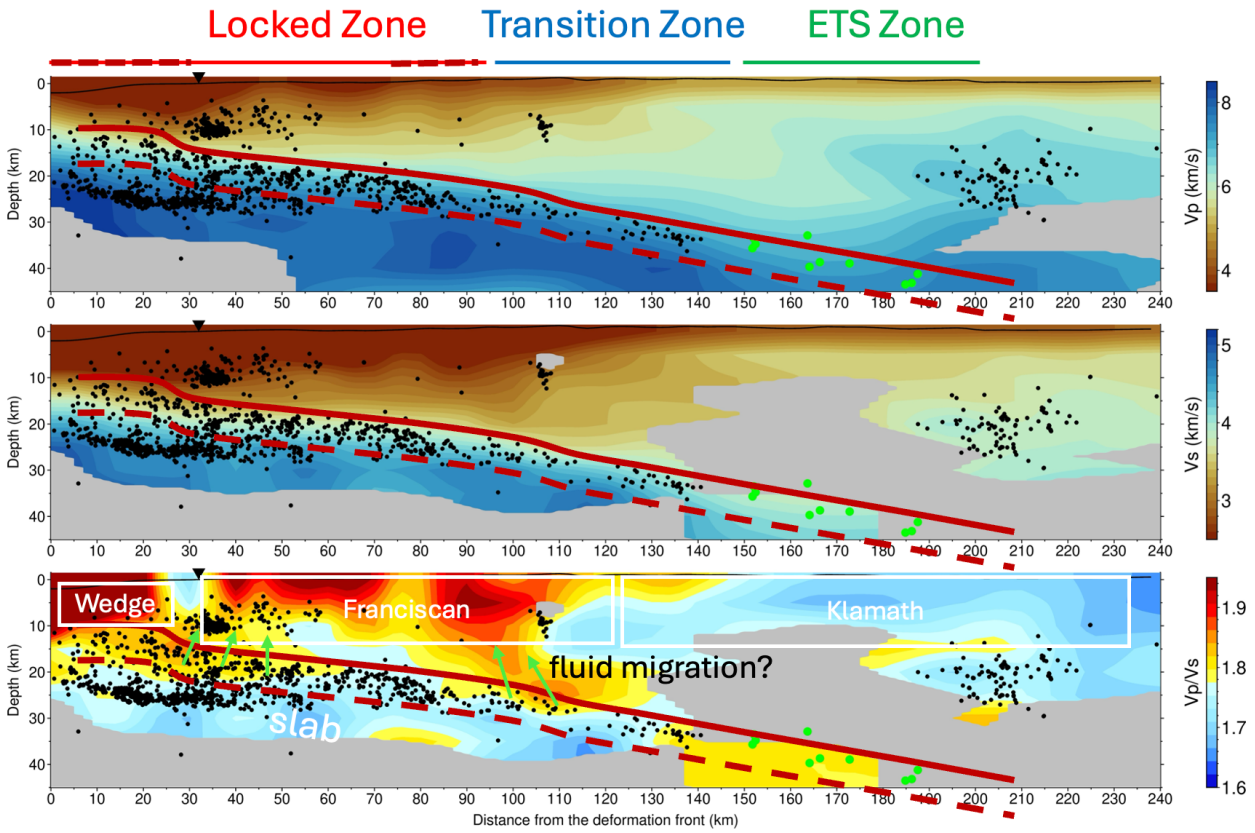

Figure 2. Along-dip cross-sections of our new Vp, Vs, and Vp/Vs models and relocated regular earthquakes and low-frequency earthquakes showing spatial variations in material properties in the subducted Gorda slab and the overlying North America plate. The black line in Fig. 1 shows where the profile is. Black and green dots represent relocated regular earthquakes and low-frequency earthquakes, respectively. The approximate ranges of the locked zone, transition zone, and ETS zone are shown at the top of the model cross-sections. We placed dashed lines at the top and bottom of the locked zone to emphasize that the locking state at the shallow part of the megathrust, primarily offshore, and the exact location of the downdip end of the fully/highly locked zone are not well constrained. We manually outline the top of slab interface by the solid red line. The dashed red line is 6 km below the solid red line and the slab crust is approximately outlined by the two red lines. In the Vp/Vs panel, the geological structure at the top of the North America plate is approximately outlined, including the accretionary wedge, the Franciscan stratum, and the Klamath stratum. Green arrows represent potential channels of fluids migrating from slab crust to the overlying North America crust. Black triangle, deformation front; thin black line near the surface, bathymetry and topography. The regions with poor resolution estimated from checkerboard test are masked.

In the model cross-sections shown in Fig. 2, we manually outline the slab interface (i.e., solid red line) based on relocations of regular earthquakes and LFEs and velocity models. We assume the slab crust is about 6 km thick (i.e., between solid and dashed red lines). Within the slab crust, downdip variations in Vp/Vs can be seen. The Vp/Vs values in the slab crust decrease substantially from the locked zone (1.8-1.86) to the transition zone (1.72-1.76). Although the Vs and Vp/Vs models have no or weak resolution in the episodic tremor and slow slip (ETS) zone where LFEs are located, the Vp model is well resolved in the ETS zone and shows apparently low Vp. The slab mantle shows low Vp/Vs values, primarily less than 1.76. The velocity model in the overlying North America crust shows strong lateral variations, which are well spatially correlated with the geological structure. In general, Vp and Vs increase eastward from the offshore accretionary wedge to onshore Franciscan complex and further increase to the Klamath terrane, while the Vp/Vs model shows a reverse pattern. The accretionary wedge, in direct contact with the underlying slab crust, has extremely low velocities and extremely high Vp/Vs (>2.0), indicating it is a fluid-rich, sedimentary region. The Franciscan complex has moderately low Vp and Vs, and high Vp/Vs of 1.8-1.95. The Klamath terrane has relatively high velocities and Vp/Vs values of about 1.64-1.78. High-Vp/Vs anomalies connecting the top of the slab and the overlying North America crust are imaged. One is below the deformation front and is associated with strong seismicity. The other one is located at the downdip end of the locked zone and the updip end of the transition zone. These high-Vp/Vs anomalies appear to represent channels of fluids migrating from the subducted slab crust to the overlying North America crust.

3.2 Relocations of 2021 and 2022 M6 Earthquake Sequences

The 2021/12/20 M6 Petrolia and 2022/12/20 Mw 6.4 Ferndale sequences caused significant building and infrastructure damage and gas and power outages (Stein et al., 2023). The ruptured faults of the onshore subevent of the 2021 M6 and the 2022 M6 were unknown prior to the M6 sequences. Fig. 3 shows map view and cross-sections of our relocations of the M6 sequences in the template matching catalogs of Yeck et al. (2023) and Shelly et al. (2024), along with our Vp/Vs model. Relocating the M6 sequences using our 3D velocity model significantly improved event locations, especially absolute event locations.

The 2022 M6 mainshock occurred at the top of the Gorda slab crust and most of its aftershocks occurred within the slab crust (Fig. 3b), same as the 3D velocity model based location result of Guo et al. (2025) for the 2022 mainshock and aftershocks from the NCEDC catalog. The 2021 onshore M6 and most of its aftershocks occurred at the top of slab mantle with low Vp/Vs, whereas a small cluster occurred at the top of slab crust, spatially close to the 2021 aftershocks (Fig. 3c). The 2021 offshore M6 and its aftershocks are vertically distributed at depths of 15 to 25 km, clearly delineating the deep part of the Mendocino fault (Fig. 3d). The Mendocino fault is also imaged as a sharp boundary with strong contrast in Vp/Vs across the fault, extending from the surface to ~20 km depth, and the 2021 offshore mainshock and aftershocks are located at the bottom of this Vp/Vs contrast, suggesting a deep seismogenic zone of the Mendocino fault. This could be attributed to increased fluid pressures in the fault zone originating from the accretionary prism of the Gorda plate on the northern side of the Mendocino fault.

It's interesting to see that most of the 2021 onshore aftershocks appear to be distributed within the area of low Vp/Vs (Fig. 3c) and high coseismic slip, although how this mainshock ruptured is not well determined (Yeck et al., 2023). In comparison, most of the 2021 offshore aftershocks and most of the 2022 aftershocks are distributed surrounding the areas of high Vp/Vs (Figs. 3b, 3d) and high coseismic slip (Yeck et al., 2023; Shelly et al., 2024). Understanding the relationship between fault-zone material properties and the distribution of aftershocks with respect to the mainshock rupture is in progress.

Relocations of the events between 2021/12/1 and 2023/6/1 in the deep learning catalog of Yoon & Shelly (2024) show similar patterns as that from relocations of the Yeck et al. (2023) and Shelly et al. (2024) catalog events. However, the events in the deep learning catalog are distributed much more diffusely than the events in template matching catalogs. This deep learning catalog appears to contain many unreal events, which may be due to false arrival picks and event associations.

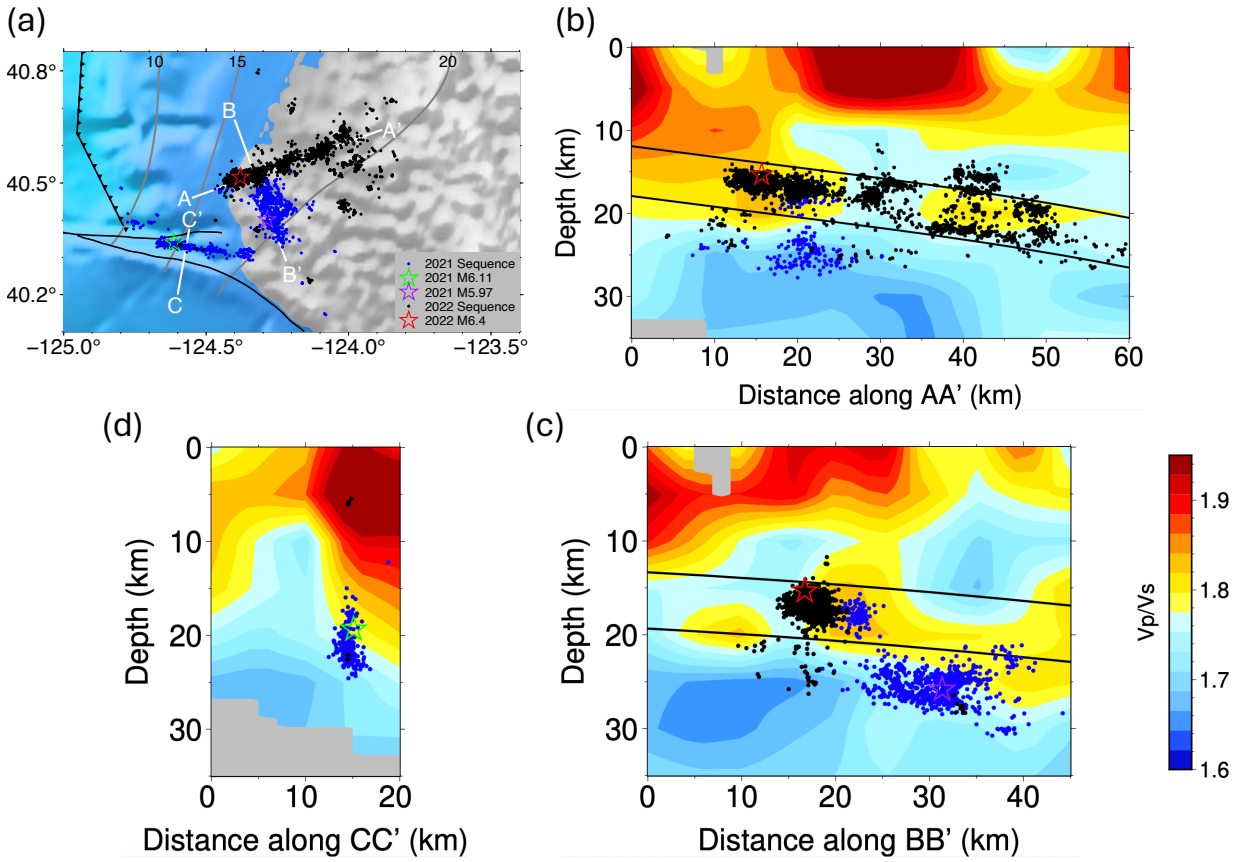

Figure 3. Our relocations of the 2021 M6 Petrolia earthquake sequence of Yeck et al. (2023) and the 2022 M6 Ferndale earthquake sequence of Shelly et al. (2024), shown in map view and cross-sections along the profiles AA', BB', and CC'. Blue dots, 2021 sequence; Black dots, 2022 sequence. The 2021 offshore and onshore M6 and the 2022 M6 are shown as stars. Events within 10 km of the profile are shown. The images in the cross-sections are our Vp/Vs model. The Slab2 plate interface model is shown as the shallower black line and the other black line is 6 km below the Slab2 model. These two lines approximately outline the slab crust.

4. Significance of Results

We developed high-resolution velocity models for the MTJ region using advanced seismic tomography method with abundant local earthquake data. Our model helps to better delineate megathrust fault structure and characterize spatial variations in material properties in the subducted slab and the overlying North America crust. Our model shows downdip variations in material properties from the locked zone to the ETS zone, which are likely correlated with downdip rheologic transitions of the megathrust fault. Our new model is also valuable in other aspects, such as estimating basin depths, determining earthquake locations and source mechanisms, and simulating ground motions, all of which are important for seismic hazard assessment. Our high-resolution velocity model and high-precision relocations of the 2021 M6 Petrolia and 2022 Mw 6.4 Ferndale sequences better delineate fault structures of these M6 earthquakes and show spatial relationships between mainshock rupture, aftershock distribution, and Vp/Vs structures. Our velocity model and our earthquake relocations are also valuable for the future update of the Community Fault Model, especially the megathrust fault and the faults ruptured by the 2021 and 2022 M6 earthquakes that were unknown prior to the M6 sequences.

5. Presentations

Guo, H. (2025, 09). Improving 3-D Seismic Velocity Structure of the Mendocino Triple Junction Region in Southern Cascadia with Densified Permanent Seismic Network Data. Poster Presentation at 2025 SCEC Annual Meeting. SCEC Contribution 14848.

Guo, H. (2025, 10). Imaging Along-Dip Variations in Material Properties of the Subducted Crust and Their Link to Megathrust Fault Coupling in Southern Cascadia. Oral Presentation at 2025 CRESCENT Offshore Observations Topical Workshop, Incoming Structure Session, held at the University of Washington, Seattle.

Guo, H. (2025, 10). Downdip variations in material properties of the subducted Gorda slab crust near Mendocino Triple Junction from high-resolution seismic tomography. Poster Presentation at 2025 CRESCENT Annual Meeting held at the University of Washington, Seattle.

6. References

Delph, J. R., A. M. Thomas, A. C. Stanciu, K. Aslam, A. Chatterjee, and V. Sassard (2022). SCENTAR: A High-Density Nodal Array to Study the Structure and Seismogenic Behavior of the Southern Cascadia Forearc, Seismol. Res. Lett. 94, 496–506, doi:10.1785/0220220251

Guo, H., Atterholt, J. W., McGuire, J. J., & Thurber, C. (2025). Evidence for low effective stress within the crust of the subducted Gorda plate from the 2022 December M w 6.4 Ferndale earthquake sequence. Seismological Research Letters, 96(3), 1504-1520. https://doi.org/10.1785/0220240078

Guo, H., McGuire, J. J., & Zhang, H. (2021). Correlation of porosity variations and rheological transitions on the southern Cascadia megathrust. Nature Geoscience, 14(5), 341–348. https://doi.org/10.1038/s41561-021-00740-1

Guo, H., & Zhang, H. (2017). Development of double-pair double difference earthquake location algorithm for improving earthquake locations. Geophysical Journal International, 208(1), 333–348. https://doi.org/10.1093/gji/ggw397

Hayes, G. P., Moore, G. L., Portner, D. E., Hearne, M., Flamme, H., Furtney, M., & Smoczyk, G. M. (2018). Slab2, a comprehensive subduction zone geometry model. Science, 362(6410), 58-61. DOI:10.1126/science.aat4723

Levander, A. Seismic and Geodetic Investigations of Mendocino Triple Junction Dynamics (International Federation of Digital Seismograph Networks, 2007); https://doi.org/10.7914/SN/XQ_2007

NCEDC (2014), Northern California Earthquake Data Center. UC Berkeley Seismological Laboratory. Dataset. doi:10.7932/NCEDC.

Plourde, A. P., Bostock, M. G., Audet, P. & Thomas, A. M. Low-frequency earthquakes at the southern Cascadia margin. Geophys. Res. Lett. 42, 4849–4855 (2015). https://doi.org/10.1002/2015GL064363

Share, PE., Guo, H., Thurber, C.H., Zhang, H., & Ben-Zion, Y. (2019). Seismic imaging of the southern California plate boundary around the south-central Transverse Ranges using double-difference tomography. Pure Appl. Geophys. 176, 1117-1143. doi.org/10.1007/s00024-018-2042-3

Shelly, D. R., D. E. Goldberg, K. Z. Materna, R. J. Skoumal, J. L. Hardebeck, C. E. Yoon, W. L. Yeck, and P. S. Earle (2024). Subduction intraslab-interface fault interactions in the 2022 Mw 6.4 Ferndale, California, earthquake sequence, Sci. Adv. 10, no. 10, eadl1226, doi: 10.1126/sciadv.adl1226

Stein, R. S., S. Toda, C. Rollins, and V. Sevilgen (2023). December 2022 California earthquake ruptured unknown fault: An analysis, Temblor, doi:10.32858/temblor.294

Toomey, D. R., Allen, R. M., Barclay, A. H., Bell, S. W., Bromirski, P. D., Carlson, R. L., ... & Wilcock, W. S. (2014). The Cascadia Initiative: A sea change in seismological studies of subduction zones. Oceanography, 27(2), 138-150. https://www.jstor.org/stable/24862164

Yeck, W. L., D. R. Shelly, K. Z. Materna, D. E. Goldberg, and P. S. Earle (2023). Dense geophysical observations reveal a triggered, concurrent multi-fault rupture at the Mendocino Triple Junction, Commun. Earth Environ. 4, no. 1, 94, doi:10.1038/s43247-023-00752-2

Yoon, C. E., and D. R. Shelly (2024). Distinct yet adjacent earthquake sequences near the Mendocino triple junction: 20 December 2021 Mw 6.1 and 6.0 Petrolia, and 20 December 2022 Mw 6.4 Ferndale, Seism. Rec. 4, no. 1, 81–92. https://doi.org/10.1785/0320230053

Zhang, H., and C. H. Thurber (2003). Double-difference tomography: The method and its application to the Hayward fault, California, Bull. Seismol. Soc. Am. 93, no. 5, 1875–1889. https://doi.org/10.1785/0120020190